ELSEVIER

Biophysical Chemistry 58 (1996) 303–312

Biophysical Chemistry

Fluorescence and Monte Carlo conformational studies of the (1–15) galanin amide fragment

Wiesław Wiczk *, Piotr Rekowski, Gotfryd Kupryszewski, Jacek Łubkowski, Stanisław Oldziej, Adam Liwo

Faculty of Chemistry, University of Gdańsk, Sobieskiego 18, 80-952 Gdańsk, Poland

Received 9 March 1995; revised 31 May 1995; accepted 31 May 1995

Abstract

Galanin (GAL) is a 29 amino acid C-terminally aminated linear neuropeptide showing diverse biological activities. The N-terminal (1–15)GAL-NH_2 fragment was shown to have a very high affinity to the galanin receptor. In this work we describe the results of a combined fluorescence and Monte Carlo studies, the latter carried out using the ECEPP/3 force field with and without including hydration, on the (1–15)GAL-NH_2 fragment. Using the time-domain technique we measured fluorescence decay times of the tyrosine residue in position 9. Based on the Förster energy transfer theory we calculated the distance and distance distribution between the Trp^2 (acceptor) and Tyr^9 (donor) aromatic side chains. The distance obtained was about 10.5 Å and half-width, hw, of the distance distribution was 5.6 Å. This results were found to be in good agreement with the chromophore distances calculated for the low-energy solution confirmations obtained in Monte Carlo simulations. All the low-energy conformations obtained in the absence of water were almost all-helical with the exception of a few C-terminal residues. In contrast, none of the low-energy solution conformations contained any significant amount of secondary structure. These findings are in agreement with the results of earlier CD and NMR conformational studies of galanin in water and non-aqueous solvents. On the other hand, the conformations obtained in the presence of water turned out to be largely compact in the N-terminal hydrophobic part. This explains the relatively short distance between chromophores and narrow distance distribution obtained in fluorescence measurements.

Keywords: Galanin; Energy transfer; Molecular mechanics; Tyrosine fluorescence

1. Introduction

Galanin (GAL) is a linear 29 amino acid C-terminally aminated neuropeptide isolated from the gut and the brain. It displays several important biological functions being a potent inhibitor of the glucose-induced insulin release in the dog [1], inhibiting acetocholine release in the rat ventral hippocampus [2], stimulating the human growth hormone release [3], potentiating the effects of morphine [4] and potently stimulating the feeding behavior when injected into the hypothalamus or lateral ventricles [5]. The amino acid sequence of galanin is known in five species: pig [6], rat [7], cow [8], chicken [9] and man [4]. As shown in Fig. 1, the sequences of these galanins are identical at the first 15 N-terminal amino acid residues. The structure-activity relationship of galanin

* Corresponding author.

SSDI 0301-4622(95)00104-2

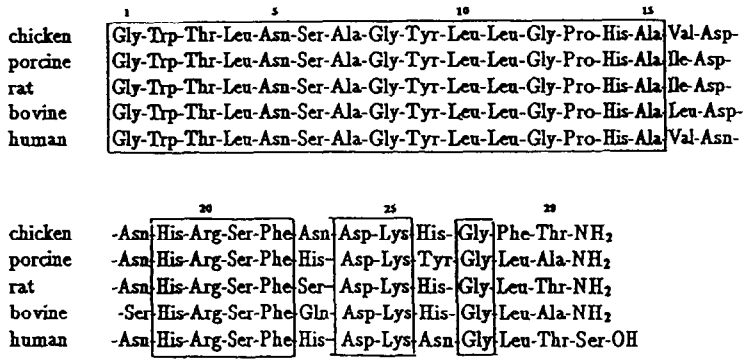

Fig. 1. Amino acid sequences of galanins from different species. Regions conserved in all the species are boxed (for reference see text).

and its analogues have shown the N-terminal fragments to have a very high affinity to the galanin receptor in the rat pancreas, brain [10], spinal cord [11], hippocampus [12], and hypothalamus [13]. The equilibrium binding constants (K_D) for galanin and its N-terminal fragments are shown in Table 1. These data suggest that almost the entire biological activity is associated with the N-terminal (1–15) fragment of galanin. The (16–29)galanin fragment alone does not bind to the receptor in the 10^{-10}–10^{-4} M concentration range [14]. The conformation of galanin in both aqueous and nonaqueous solution was studied by the NMR [15], CD and IR spectroscopy [16] and molecular dynamics [17]. These investigations have shown that while the peptide has virtually no secondary structure in aqueous solution, all-helical conformations are dominant in nonaqueous solvents such as trifluoroethanol.

In this work, using time-resolved fluorescence spectroscopy and theoretical Monte Carlo simulations, we carried out a conformational study of the (1–15)GAL-NH_2 fragment (the conservative fragment for all galanins with high affinity to the galanin receptor). The fluorescence measurements were carried out in aqueous solution, while both aqueous and non-aqueous environment was simulated in theoretical calculations.

Table 1
Linear N-terminal galanin fragments as ligands at the rat hypothalamic galanin receptor (from [14])

Receptor ligand	K_D (μM)
(1–29)GAL	0.0008
(1–16)GAL	0.007
(1–15)GAL	0.20
(1–12)GAL	3.00

2. Materials and methods

2.1. Synthesis

The (1–15) fragment of porcine galanin amide, (1–15)GAL-NH_2, was obtained by the solid phase peptide synthesis [18,19]. The α-amino group of the amino acids was protected by the *t*-butyloxycarbonyl group. For side chain protection the following protecting groups were used: L-arginine (*p*-toluensulphonyl), L-lysine (2-chlorobenzyloxycarbonyl), L-tryptophan (formyl), L-histidine (benzyloxymethyl), L-serine, L-threonine (benzyl ether), L-tyrosine (2,6-dichlorobenzyl ether).

The first amino acid was attached to methylbenzhydrylamino resin (MBHA) using DCC as coupling reagent. The synthesis of fully protected peptides on the resin was carried out according to standard procedures. The peptide was deprotected and cleaved from the resin by liquid hydrogen fluoride. The crude peptide was desalted on a Sephadex G-25 F column and then purified by RP preparative HPLC on a Vydac C-18 column. The details of the syntheses are given elsewhere [20].

The (1–15) fragment of galanin amide in which Trp in position 2 was replaced by Ile, (Ile^2)(1–15)GAL-NH_2, was obtained by solid phase peptide synthesis (continuous flow) on a Milligen 9050 synthesizer using Fmoc strategy on TentaGel S-Ram resin (Rapp Polymer). The following side chain protections were applied: *t*-butyl group for L-threonine

and L-tyrosine and trityl group for L-histidine and L-asparagine. The attachment of the first amino acid to the resin and coupling reactions were carried out using diisopropylcarbodiimide (DIPCI) in presence of 1-hydroxybenzotriazole (HOBt). The peptide was deprotected and cleaved from the resin by mixture of trifluoroacetic acid (88%), i-Pr_3SiH (2%), phenol (5%) and water (5%) and purified by RP preparative HPLC on a Kromasil C-18 column (2.5 × 25 cm, 10 μm). The peptide was pure (more than 99.5% by analytical HPLC) and displayed the expected amino acid composition.

2.2. Fluorescence studies

The steady-state spectra were obtained on a Perkin-Elmer LS-50 B spectrofluorimeter with a 2.5-nm bandwidth for excitation and emission. The excitation wavelength was 275 nm for tyrosine and tryptophan and 295 nm for tryptophan only. The quantum yields were measured relative to a value of 0.14 for tyrosine in water at room temperature [21].

Fluorescence decays were collected by time-correlated single photon counting technique on an Edinburgh Analytical Instrument type CD-900 fluorimeter interfaced with an IBM PC AT. The excitation source was a flash lamp filled with 0.5 atm hydrogen, operated at 40 kHz with about 6.5 kV across a 1 mm electrode gap. The half width of the instrument response was 1.2 ns. The excitation (270 nm) and emission wavelengths (290 nm) were selected by means of monochromators (about 5 nm band width).

In steady-state measurements sample concentration was about $5 \cdot 10^{-5}$ M and $1 \cdot 10^{-4}$ M in time-resolved experiments.

Fluorescence decays from the sample and the reference (Ludox, observation wavelength 290 nm) were measured to 10^4 counts in the peak. The counting rate did not exceed 2% of the lamp repetition rate. The decay curves were stored in 1024 channels of the 0.054 ns/channel.

3. Theory and calculations

The details of data analysis has been described elsewhere [22,23]. Here we present only a brief description.

If the single acceptor is not rigidly fixed in space with respect to the donor coordinates, there will be a range of donor–acceptor distances. While the decay of the donor corresponding to each donor–acceptor separation will still be a single exponential, the overall observed donor decay will contain contributions reflecting the range of all possible donor–acceptor distances thus being more complex than a single exponential. It is this deviation from single-exponential behavior that provides a measure of the donor–acceptor distance distributions. The analysis of distance distribution involved two steps. In the first step, we analyzed the fluorescence decay of donor alone in the peptide by a sum of exponentials:

$$I_D(t) = \sum_i \alpha_i \exp(-t/\tau_i) \quad (1)$$

where α_i and τ_i are the amplitude and lifetimes of the ith component, respectively. The large number of data points from each single-photon counting measurement permits the judgement of quality of data fit beyond the simple χ^2 statistics commonly

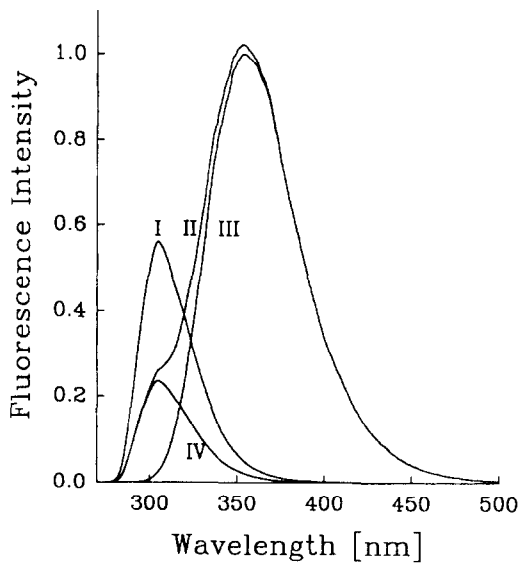

Fig. 2. Fluorescence spectra of galanin fragments measured in acetate buffer at pH = 5.6 at room temperature. I: the spectrum of the (Ile^2)(1–15)GAL-NH_2 fragment (donor, λ_{ex} = 275 nm); II: the spectrum of (1–15)GAL-NH_2 fragment (donor–acceptor pair, λ_{ex} = 275 nm); III: The same as II but at λ_{ex} = 295 nm (emission of tryptophan only) normalized to curve II at 400 nm; IV: the difference between curves II and III (tyrosine emission contribution to curve II).

used. We used reduced χ^2, weighted residuals, and autocorrelations of residuals to judge the fit of Eq. (1) to experimental data [24].

In the second step, we analyzed the donor decay of the donor–acceptor pair in the peptide using distance distribution according to:

$$I_{DA}(t) = \int P(r) \sum_i \alpha_i \exp\left\{ -\frac{t}{\tau_i}\left[1 + \left(\frac{R_0}{r}\right)^6\right]\right\} dr \quad (2)$$

where $P(r)$ defines the shape of distribution, and the integral covers all donor–acceptor distances over which energy transfer occurs.

The function $P(r)$ is defined so, that $P(r)dr$ is a probability that in a given macromolecule the donor–acceptor distance, r, is in the interval $(r, r + dr)$. The function $P(r)$ is parametrized assuming the Gaussian model:

$$\begin{cases} P(r) = Z^{-1}\exp[-0.5(r - R_{av})^2/\sigma^2] & \text{for } r_{min} < r < r_{max} \\ P(r) = 0 & \text{elsewhere} \end{cases} \quad (3)$$

where Z is the normalization factor:

$$Z = \int_{r_{min}}^{r_{max}} \exp[-0.5(r - R_{av})^2/\sigma^2] \text{ for } r_{min} < r < r_{max}. \quad (4)$$

The average distance and standard deviation of the untruncated Gaussian function are R_{av} and σ, respectively. The standard deviation is related to the half-width of the distribution (i.e. the full width at half-maximum height) by $hw = 2.354\sigma$. The Förster critical distance R_0 was calculated as described elsewhere [25].

In our analysis we assume $\kappa^2 = 2/3$ due to the range of conformation and the possibility of the rotational diffusion and the mixed polarization of the chromophores [26].

The rotational correlation times of 0.56 ns that describe the motion of Trp itself and another 4.2 ns which is due to the overall motion of the peptide indicating a high mobility of the Trp residue in pig galanin [16]. Such comparatively unrestricted rotation of tryptophan was also reported for melittin [27,28] and monellin [27]. Because the (1–15)galanin fragment has a size similar to that of melittin [29] and the tyrosine residue in galanin is exposed to the solvent [16], it can be assumed that the rotation of the tyrosine chromophore is quite unrestricted, as for tryptophan in melittin and galanin. A rapid chromophore rotation results in a dynamic averaging of the κ^2 value which justifies our choice of $\kappa^2 = 2/3$.

We used the known amplitude (α_i) and lifetime (τ_i) of donor decay in the absence of acceptor obtained in Eq. 1 as the input to fit the data with Eq. 2 to determine the distance distribution parameters. The goodness of fit was judged exactly as in the case of donor-only decay.

The energy-transfer efficiency (E_T) can be related to the quantum yield of donor fluorescence alone (η_D) and fluorescence quantum yield of the donor in the D–A pair (η_{DA}).

$$E_T = 1 - \frac{\eta_{DA}}{\eta_D} = \frac{R_0^6}{R_0^6 + R_{av}^6}. \quad (5)$$

3.1. Monte Carlo simulations

The exploration of the conformational space of galanin (1–15) fragment was carried out with the use of the electrostatically-driven Monte Carlo (EDMC) method [30–36]. Briefly, this method is based on perturbing an arbitrary starting energy-minimized conformation, subsequent energy minimization of the perturbed conformation and comparison of the resulting energy with the energy of the starting conformation. Some of the perturbations are directed at the optimization of the electrostatic interaction within the polypeptide chain. If the energy of the new conformation appears lower, the new conformation is accepted; otherwise the Metropolis test is performed in order to accept or reject the new conformation. The new conformation replaces the starting one, if accepted, and the procedure is repeated. The process is iterated until either no new conformations can be found or a sufficient number of conformations have been accepted. This method was shown to be able to find the global energy minimum (GME) of small peptides like enkephalin [30] or even peptides of medium size, like melittin [31].

Conformational energy was evaluated using the ECEPP/3 (empirical conformational energy pro-

gram for peptides) force field [37]. In order to simulate the experimental conditions, in one series of simulations we considered hydration contribution to energy using a model with a 1.4 Å radius solvent sphere with atomic solvation parameters optimized using nonapeptide data (SRFOPT) [33,34]. In order to study the effect of environment on galanin conformation, another series of simulations was carried out without including hydration contribution; this corresponds to the receptor or non-polar-solvent environment.

In both series of simulations starting conformations with the following backbone geometries were assumed: (i) α-helical, (ii) 3_{10}-helical, (iii) a series of conformations with a two-strand antiparallel β-sheet with different types of β-turns at Ala^7–Gly^8, (iv) an extended conformation as a reference. Conformations of type (iii) were generated based on the results of secondary- structure prediction obtained from the Chou–Fasman method [38,39], using the PREDICT program [40]. Each of the EDMC runs was terminated after 50 energy-minimized conformations were accepted. The parameters controlling the EDMC runs were as follows: temperature = 300 K; maximum number of allowed repetitions of the same minimum = 50; maximum number of rejected conformations until the backtrack-type motion is attempted = 100. A total of 800 conformations were obtained in each series of simulations.

In order to group the conformations obtained into families of similar conformations, the minimal-tree algorithm of cluster analysis was employed [41]. The root mean square (RMS) deviation between the backbone heavy atoms at an optimum superposition was taken as a measure of the difference between two conformations. The RMS cut-off was 1.0 Å.

The distance between the Trp^2 and Tyr^9 chromophores was calculated as the distance between the geometric centers of the indole moiety of tryptophan and the tyrosine phenol ring.

4. Results

4.1. Fluorescence studies

4.1.1. Steady-state measurements

The uncorrected emission spectra of the donor (Ile^2)(1–15)GAL-NH_2 and donor–acceptor pair (1–15)GAL-NH_2 measured in acetate buffer (pH = 5.6) are shown in Fig. 2. The emission spectrum of the donor is characteristic of tyrosine with the emission maximum at about 303 nm (I). The emission spectrum of the donor–acceptor pair (D–A) (II) at an excitation wavelength of 275 nm is a sum of emissions of tyrosine (donor) and tryptophan (acceptor). At the 295 nm excitation tryptophan is only excited and its emission spectrum after normalization with respect to the D–A pair for 400 nm emission is shown by curve (III). The difference between two spectra, (II) – (III), represents the share of the donor fluorescence in the overall emission of the D–A pair (IV). The donor emission in the D–A pair, corrected for the absorption of the acceptor, is about half that of the donor alone. The fluorescence quantum yield of the donor is 0.030, whereas in the D–A pair it is 0.0117. Almost two-fold quenching of the tyrosine fluorescence is due to the energy transfer from tyrosine to tryptophan.

The average distance R_{av} calculated from the steady-state measurements using Eq. 5 is 10.3 Å. The Förster critical distance (R_0) used to calculate the distance and the distance distribution was 11.1 Å, which is between values 10.8 Å given by Bodanszky for oxytocin [42] and 11.8 Å given by Kilhoffer for VU-6 calmodulin [43].

In general, the energy transfer can be measured either from the donor emission quenching or the sensitized acceptor fluorescence. In practice, the majority of the energy transfer experiments are carried out by measuring the donor fluorescence quenching since the overall emission results from directly absorbed radiation. When the energy transfer is measured based on the sensitized acceptor fluorescence one should take account of the emission fraction due to the direct excitation of the acceptor. The measurements of the donor emission are convenient in time-resolved experiments in which the share of the acceptor cannot be readily added or subtracted [25,44].

4.1.2. Time-resolved measurements, multiexponential analysis of time-resolved fluorescence decay data

The fluorescence decay of the donor when isolated or in the D–A pair, shown in Fig. 3, was analyzed as a sum of exponents.

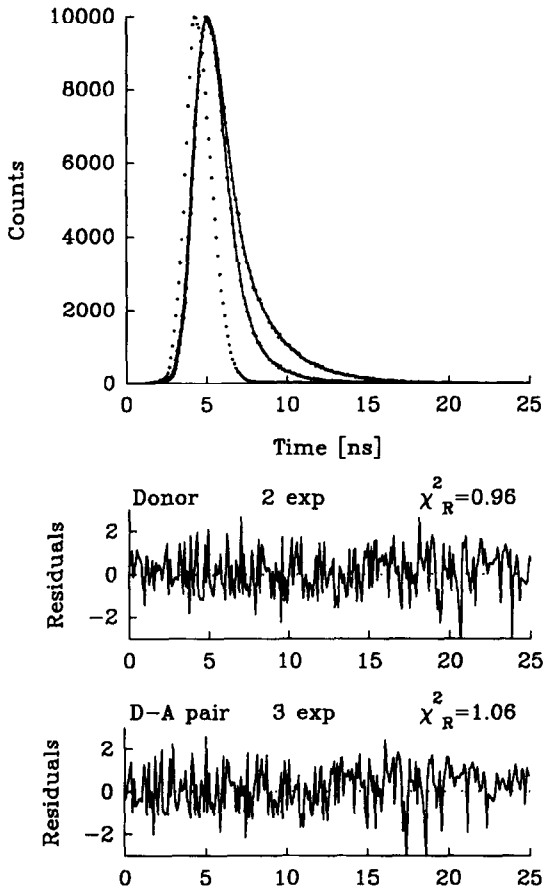

Fig. 3. Upper part: fluorescence decay curve for tyrosine in donor-only (upper curve), donor–acceptor pair (middle curve) and lamp profile (lower curve). Solid lines represent the best-fit double (donor) and triple (donor–acceptor) decay curves. Lower part: weighted residuals.

The results obtained are given in Table 2. A sum of two exponents (for donor) and three exponents (for D–A pair) had to be used for describing the fluorescence decay with an adequate fit. It should be pointed out that although the share of the third component with the longest lifetime in D–A pair is the least (below 1%, Table 2), it improves the fit of the calculated decay to the experimental curve. Since the two components contribute more than 99% of the detected signal, they basically define the shape of the decay. The parameters of double exponential decay times for an isolated donor, $\tau_1 = 0.56$ ns and $\tau_2 = 2.30$ ns, closely correspond to decay times reported by Ross [45] for tyrosylglycine and N-acetyltyrosine amide.

Such an empirical analysis of the decay curves enables the averaged properties of the system to be obtained. The data were analyzed using Eqs. 1 and 2 with assuming a Gaussian distribution of the D–A distances (Eqs. 3 and 4). This model results in a good fit to the data, with χ^2_R amounting to 1.37. While these values are not as low as for the three-exponential fit (Table 2), this model has only two floating parameters (R_{av} and hw), whereas the three-exponential model involves six adjustable parameters (three τ_i and three α_i). It is also unlikely that the D–A distribution can be precisely described by any of these models since the linker is not infinitely long [46]. For the sample dealt with the best fit yielded the following parameters: $R_{av} = 10.6$ Å and hw = 5.6 Å with $\chi^2_R = 1.37$ (Fig. 4). When the same set of data were refitted with hw fixed at 1 Å corresponding to a narrow distribution, there was a 27-fold increased in χ^2_R to 36.5. When the data were refitted with hw fixed at 25 Å, corresponding to a wide distribution, there was 11-fold increase in χ^2_R to 15.3, indicating that the data were incompatible with the narrow and wide distribution. Fig. 5 shows the recovered distance distribution $P(r)$.

Finally we examined the uncertainties in R_{av} and hw. This was accomplished by fitting the data with one parameter fixed while the other was varied so as to minimized χ^2_R. If the parameter is determinable, χ^2_R should vary considerably when changing the

Table 2
Multiexponential analysis of time-resolved fluorescence decay data of tyrosine measured in acetate buffer (pH = 5.6) at room temperature. Excitation wavelength 270 nm, emission 290 nm (5-nm band width)

Sample	α_i	τ_i	χ^2_R
(Ile^2)(1–15)GAL-NH$_2$	1.0000	1.89	8.93
(donor)	0.6805	0.56	
	0.3135	2.30	0.96
(1–15)GAL-NH$_2$	1.0000	1.05	6.71
(donor–acceptor pair)	0.8318	0.53	
	0.1682	1.63	1.63
	0.7365	0.32	
	0.2565	1.24	
	0.0070	3.18	1.06

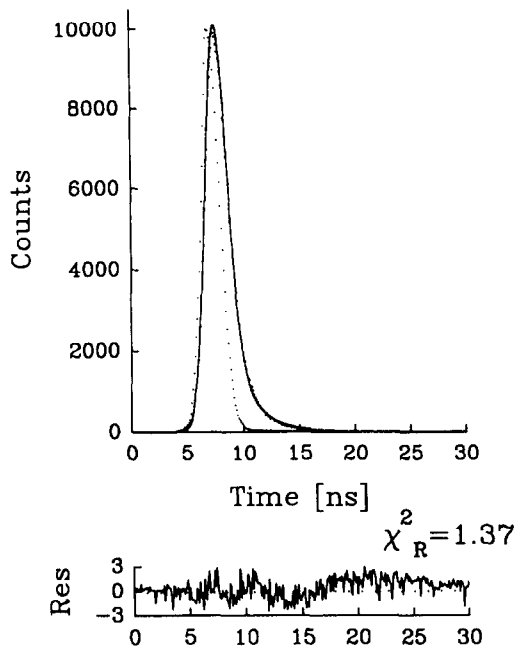

Fig. 4. Upper part: fit to the fluorescence decay data of the donor–acceptor pair using Eq. 2 with a Gaussian-type distance distribution (Eq. 3) (solid line fitted to upper points) and the lamp profile (lower points). The obtained distance distribution parameters are R_{av} = 10.6 Å and hw = 5.6 Å. Lower part: weighted residuals.

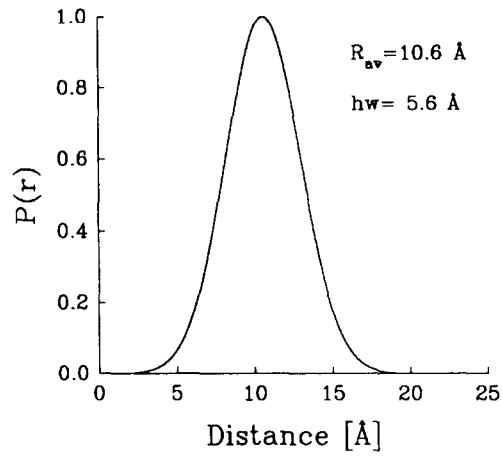

Fig. 5. The calculated distance distribution curve (Eq. 3) between tyrosine and tryptophan residues of the (1–15)galanin fragment.

parameter value and a deep minimum should appear that corresponds to the best-fittings value of this parameter. If, however, the parameter cannot be determined with satisfactory accuracy, the dependence of χ^2_R on the parameter value will be weak and minimum corresponding to the best-fitting value of the parameter will be broad. The dependence of χ^2_R on R_{av} and hw for the D–A pair is shown in Fig. 6. In both cases deep minima in the corresponding curves can be observed showing that both R_{av} and hw can be determined with a satisfactory accuracy. At the 95% confidence level $10.1 \leqslant R_{av} \leqslant 11.3$ and $5.1 \leqslant hw \leqslant 6.4$ Å.

4.2. Monte Carlo simulations

The stereoviews of the lowest-energy conformations of the (1–15)galanin fragment calculated with and without including hydration are shown in Fig. 7A and B, respectively, while the conformational states (assigned after Zimmerman et al. [47]) of the low-energy conformations (i.e. within 5 kcal/mole energy cut-off) are summarized in Table 3.

As shown, the conformations in the absence of water are almost completely helical with the exception of a few C-terminal residues. This is also the feature of most of the higher-energy conformations lying within 20 kcal/mol energy cut-off. In contrast, none of the low-energy conformations obtained with including hydration contains any significant amount of secondary structure. This is in complete agreement with CD and NMR studies of galanin in trifluoroethanol and in water [15,16].

On the other hand, the conformations obtained

Table 3
Conformational states of the lowest-energy conformations of the (1–15)galanin fragment in presence (upper part of the table) and absence of solvent (lower part of the table). (Conformational codes of the individual residues assigned according to Zimmerman et al. [47]). Only residues from 2 to 14 are included

Conformational code	Relative energy (kcal/mol)
E A D E C G B G C A D A A	0.0
E A E E C G D G C A D A A	0.43
E C A* E C A D G C A D C A	2.89
E A D E C G D G C A E* A A	3.76
A A A A A A A A A A E* C E	0.00
A A A A A A A A A A D* F C	3.48

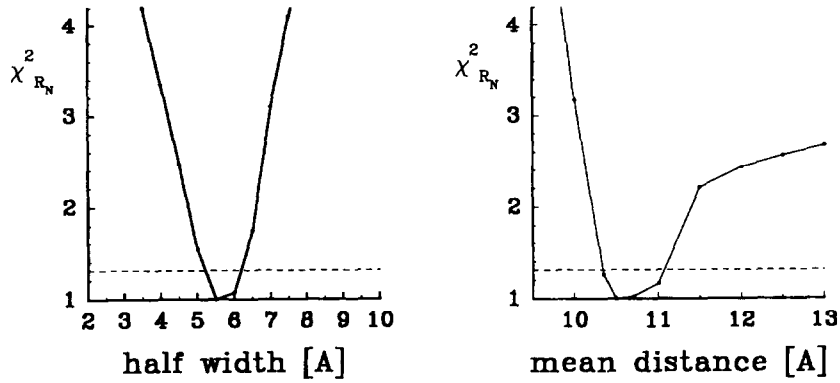

Fig. 6. Sensitivity analysis of the fits to the decay data of the (1–15)galanin fragment. Left panel: the χ^2_R value calculated for different hw. Right panel: the χ^2_R value calculated for different R_{av}. The horizontal dashed line is the χ^2_R value corresponding to the 95% confidence level.

with including hydration can be characterized by a largely extended C-terminal fragment exposed to water and a compact N-terminal fragment containing mostly hydrophobic residues that tend to form a hydrophobic cluster. In particular, the Trp^2 and Tyr^9 chromophores are spatially close.

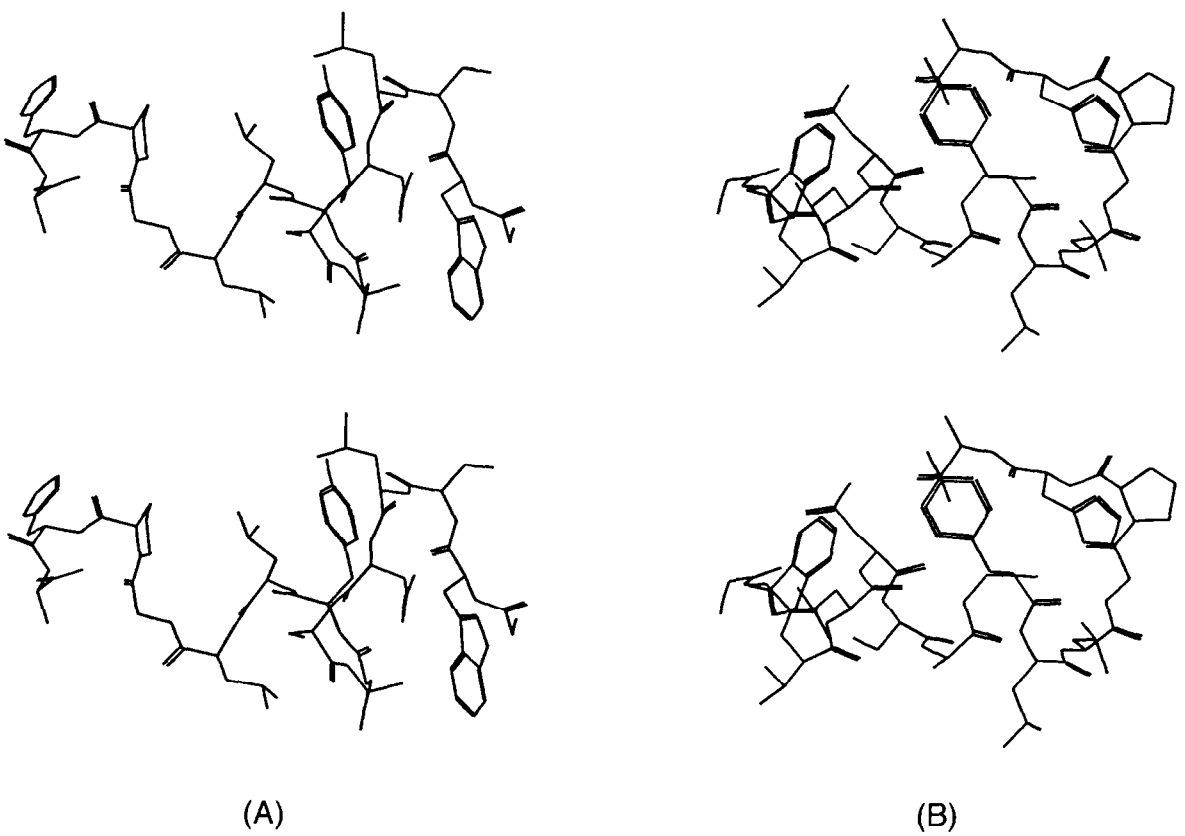

Fig. 7. Stereoview of the lowest-energy conformation of (1–15)galanin fragment obtained in Monte Carlo simulations in the presence (a) and in the absence (b) of water.

5. Discussion

The position of the tryptophan emission with a maximum around 355 nm indicates its having been exposed to the solvent. Both steady-state and time-resolved fluorescence measurements confirm the occurrence of the energy transfer from tyrosine to tryptophan. The energy transfer efficiency, E_T calculated from the fluorescence quantum yields is 0.61. The calculated mean distribution parameters are: $R_{av} = 10.6$ Å and $hw = 5.6$ Å. Using the F-test we determined that at 95% confidence level $10.1 \leqslant R_{av} \leqslant 11.3$ and $5.1 \leqslant hw \leqslant 6.4$ Å. The energy transfer efficiency calculated for these distribution parameters, $E_T = 0.57$, is comparable to that obtained from steady-state measurements. These data suggest that in the conformations of galanin in aqueous solution the aromatic tyrosine and tryptophan residues are spatially close, as also concluded from the results of theoretical simulations.

If the 8-residues fragment of galanin chain (from Trp^2 to Tyr^9) assumed fully random conformations, the distribution of chromophore distance could be expected to follow the Markov distribution of the distances in a random polymer chain. We have calculated this distribution following the procedure of Miyazawa and Jernigan ([48] Eqs. 25–31). For a random polypeptide chain of a length of 7 (the number of peptide bonds separating the chromophores) containing one glycine residue the mean distance is 18.5 Å and the half-width of the distance distribution is 20.5 Å. Both values are therefore much greater than the ones obtained in the present study. In the case of some model tetrapeptides which tend to assume random conformations, the average chromophore distance is 9 Å, and the half-width amounts to 25 Å [49], compared to the values of 11 Å and 16 Å, respectively obtained from the Markov distribution.

The above conclusion regarding galanin conformation in aqueous solution are further supported by the fact that the chromophore distances calculated for the low energy conformations obtained in the presence of water (that are compact in the N-terminal part) range from about 7.5 to about 15 Å with a maximum at 9 Å and, therefore, fully contained within the range determined from experiment (taking into account the confidence interval of both the average distance and that of the half-width of the distribution).

Acknowledgements

This work was supported by Polish State Committee for Scientific Research (KBN) under grants BW/5300-5-0021-3 (to St. Oldziej and A. Liwo) and Fogarty International Center grant No. SRC 1 R03 TW00049-01 (to G. Kupryszewski and P. Rekowski). The authors are very grateful to Prof. H.A. Scheraga, Cornell University, for the EDMC program.

References

[1] B. Ahren, P. Arkhammar, P.O. Bergen and T. Nilsson, Biophys. Res. Commun., 140 (1986) 1059.
[2] G. Fisone, C.F. Wu, S. Consolo, O. Norstrom, N. Bryne, T. Bartfai and T. Hokflet, Proc. Natl. Acad. Sci. USA, 84 (1987) 7339.
[3] F.E. Bauer, L. Ginsberg, M. Venticou, D.J. Mackay, J.M. Burrin and S.R. Bloom, Lancet, 2 (1989) 193.
[4] Z. Wiesenfeld-Halin, X.J. Xu, M.J.M. Villar and T. Hokfelt, Neurosci. Lett., 109 (1990) 217.
[5] S.E. Kyrkouli, B.G. Stanley and S.F. Leibiwitz, Eur. J. Pharmacol., 122 (1986) 159.
[6] K. Tatemoto, A. Rökeaus, H. Jornval, T.J. McDonald and V. Mutt, FEBS Lett., 164 (1983) 124.
[7] M.E. Vrontakis, L.M. Peden, M.L. Duckworth and H.G. Fvisen, J. Biol. Chem., 262 (1987) 16755.
[8] A. Rökeaus and M. Carlquist, FEBS Lett., 234 (1988) 400.
[9] A. Norberg, R. Silward, M. Carlquist, H. Jornvall and V. Mutt, FEBS Lett., 288 (1991) 151.
[10] I. Lagny-Pourmir, A.M. Lorinet, N. Yanaihara and M. Laburthe, Peptides, 10 (1989) 757.
[11] H.J. Xu, Z. Wiesenfeld-Hallin, G. Fisone, T. Bartfai and T. Hokfelt, Eur. J. Pharmacol., 182 (1990) 137.
[12] G. Fisone, M. Berthold, K. Bedecs, A. Unden, T. Bartfai, R. Bertorelli, S. Consolo, J. Crawley, B. Martin, S. Nilsson and T. Hokfelt, Proc. Natl. Acad. Sci. USA, 86 (1989) 9588.
[13] J. Crawley, M.C. Austin, S.M. Fiske, B. Martin, S. Consolo, M. Berthold, U. Langel, G. Fistone and T. Bartfai, J. Neurosci., 10 (1990) 3695.
[14] T. Land, U. Langer, M. Low, M. Berthold, A. Udneden and T. Bartfai, Int. J. Peptide Protein Res., 38 (1991) 267.
[15] A.B.A. Wennerberg, R.M. Cooke, M. Carlquist, R. Rigler and I.D. Campbell, Biochim. Biophys. Res. Commun., 166 (1991) 1102.
[16] R. Rigler, A.B.A. Wennerberg, R.M. Cooke, A. Elofsson, L. Nilsson, H. Vogel, L.H. Holley, M. Carlquist, U. Langel, T. Bartfai and I.D. Campbell, in T. Hokfelt and T. Bartfai (Editors), Galanin, Macmillan, New York, 1988.

[17] H. De Loof, L. Nilsson and R. Rigler, J. Am. Chem. Soc., 114 (1992) 4028.
[18] R.B. Merrifield, J. Am. Chem. Soc., 85 (1963) 2149.
[19] B. Lammek, P. Rekowski, G. Kupryszewski, P. Melin and U. Ragnarsson, J. Med. Chem., 31 (1988) 603.
[20] P. Rekowski, A. Halama, P. Mucha, G. Kupryszewski, E. Poćwiartowska and K.Z. Korolkiewicz, Pol. J. Chem., 67 (1993) 237.
[21] R.F. Chen, Anal. Lett., 1 (1967) 35.
[22] P. Wu and L. Brand, Biochemistry, 31 (1992) 7939.
[23] J.R. Lakowicz, W. Wiczk, I. Gryczyński, M. Fishman and M.L. Johnson, Macromolecules, 26 (1993) 349.
[24] D.V. O'Connor and D. Phillips, Time-Correlated Single Photon Counting, Academic Press, London, 1984.
[25] J.R. Lakowicz, Principles of Fluorescence Spectroscopy, Plenum Press, New York, 1983, Chapter 10.
[26] E. Hass, E. Katchalski-Katzir and I.Z. Steinberg, Biochemistry, 17 (1978) 5064.
[27] J.R. Lakowicz, G. Laczko, I. Gryczyński and H. Cherek, J. Biol. Chem., 261 (1986) 2240.
[28] J.R. Lakowicz, H. Cherek, I. Gryczyński, N. Joshi and M.L. Johnson, Biophys. J., 51 (1987) 755.
[29] J.R. Lakowicz, I. Gryczyński, W. Wiczk, G. Laczko, F.C. Predergast and M.L. Johnson, Biophys. Chem., 36 (1990) 99.
[30] D. Ripoll and H.A. Scheraga, Biopolymers, 27 (1988) 1283.
[31] D. Ripoll and H.A. Scheraga, J. Prot. Chem., 8 (1989) 263.
[32] D. Ripoll and H.A. Scheraga, Biopolymers, 30 (1990) 165.
[33] J. Vila, R.L. Williams, M. Vasquez and H.A. Scheraga, Proteins: Struct. Function Genet., 10 (1991) 199.
[34] R.L. Williams, J. Vila, G. Perrot and H.A. Scheraga, Proteins: Struct. Function Genet., 14 (1992) 140.
[35] Z. Li and H.A. Scheraga, Proc. Natl. Acad. Sci. USA, 84 (1987) 6611.
[36] Z. Li and H.A. Scheraga, J. Mol. Struct. (THEOCHEM), 179 (1988) 333.
[37] G. Némethy, K.D. Gibson, K.A. Palmer, C.N. Yoon, G. Paterlini, A. Zagari, S. Rumsey and H.A. Scheraga, J. Phys. Chem., 96 (1992) 6472.
[38] P.Y. Chou and G.D. Fasman, Ann. Rev. Biochem., 47 (1978) 251.
[39] G.D. Fasman, in G.D. Fasman (Editor), Prediction of Protein Structure and the Principles of Protein Conformation, Plenum Press, New York, 1989, pp. 193–316.
[40] P. Prevelige and G.D. Fasman, in G.D. Fasman (Editor), Prediction of Protein Structure and the Principles of Protein Conformation, Plenum Press, New York, 1989, pp. 316–416.
[41] H. Späth, Cluster Analysis Algorithms, Halsted Press, New York, 1980, pp. 170–194.
[42] M. Bodanszky, J. Tolle, M. Bednarek and P.W. Schiller, Int. J. Peptide Protein Res., 17 (1981) 444.
[43] M.C. Kilhoffer, D.M. Roberts, A. Adibi, D.M. Watterson and J. Haiech, Biochemistry, 28 (1989) 6086.
[44] R.M. Clegg, A.J.H. Murchie, A. Zehel, C. Carlberg, S. Dickman and D.M.J. Lilley, Biochemistry, 31 (1992) 4846.
[45] J.B.A. Ross, W.R. Laws, K.W. Russlag and H.R. Wyssbrod, in J.R. Lakowicz (Editor), Topics in Fluorescence Spectroscopy, Vol. 3: Biochemical Applications, Plenum Press, New York, 1992, Chapter 1.
[46] P. Flory, Statistical Mechanics of Chain Molecules, Interscience, New York, 1969.
[47] S.S. Zimmerman, M.S. Pottle, G. Némethy and H.A. Scheraga, Macromolecules, 10 (1970) 1.
[48] S. Miyazawa and R.L. Jerningan, Macromolecules, 18 (1985) 534.
[49] W. Wiczk, I. Gryczyński, H. Szmaciński, M.L. Johnson, M. Kruszyński and J. Zboińska, Biophys. Chem., 32 (1989) 43.